

29. C. W. Macosko, *Rheology Principles, Measurements, and Applications* (Wiley-VCH, New York, 1994).
30. M. Doi, S. F. Edwards, *The Theory of Polymer Dynamics* (Oxford Univ. Press, Oxford, 1986).
31. J. Peanasky, L. L. Cai, S. Granick, C. R. Kessel, *Langmuir* **10**, 3874 (1994).
32. P. G. De Gennes, *Scaling Concepts in Polymer Physics* (Cornell Univ. Press, Ithaca, NY, 1979).
33. H. R. Brown, T. P. Russell, *Macromolecules* **29**, 798 (1996).
34. B. Crist, in *The Physics of Glassy Polymers*, R. N. Haward, R. J. Young, Eds. (Chapman & Hall, London, 1997), pp. 155–212.
35. M. C. Boyce, R. N. Haward, in *The Physics of Glassy Polymers*, R. N. Haward, R. J. Young, Eds. (Chapman & Hall, London, 1997), pp. 213–294.
36. Supported by Science Foundation of Ireland grant 00/PI.1/C028, NSF grants CMMI 07-32114 and DMI 03-28162, the Center for Nanoscale Chemical-Electrical-Mechanical Manufacturing Systems, NSF Faculty Early Career Development grant CBET 07-31930, and a U.S. Department of Energy Presidential Early Career Award for Scientists and Engineers. H.D.R. is vice president for engineering, Endotronix Inc., Peoria, IL.

## Supporting Online Material

www.sciencemag.org/cgi/content/full/1157945/DC1  
Materials and Methods  
Figs. S1 to S3  
Tables S1 and S2  
References

18 March 2008; accepted 16 September 2008  
Published online 2 October 2008;  
10.1126/science.1157945  
Include this information when citing this paper.

# Peptides Enhance Magnesium Signature in Calcite: Insights into Origins of Vital Effects

A. E. Stephenson,<sup>1\*</sup> J. J. DeYoreo,<sup>2</sup> L. Wu,<sup>2,3</sup> K. J. Wu,<sup>2</sup> J. Hoyer,<sup>4</sup> P. M. Dove<sup>1\*</sup>

Studies relating the magnesium (Mg) content of calcified skeletons to temperature often report unexplained deviations from the signature expected for inorganically grown calcite. These “vital effects” are believed to have biological origins, but mechanistic bases for measured offsets remain unclear. We show that a simple hydrophilic peptide, with the same carboxyl-rich character as that of macromolecules isolated from sites of calcification, increases calcite Mg content by up to 3 mole percent. Comparisons to previous studies correlating Mg content of carbonate minerals with temperature show that the Mg enhancement due to peptides results in offsets equivalent to 7° to 14°C. The insights also provide a physical basis for anecdotal evidence that organic chemistry modulates the mineralization of inorganic carbonates and suggest an approach to tuning impurity levels in controlled materials synthesis.

Over the past 50 years, the Mg/Ca ratio in marine cements (1–4) and calcified skeletal structures (5–9) has become a widely used proxy for reconstructing past Earth environments. Elemental proxy models for temperature and seawater chemistry begin by assuming that compositional signatures reflect environmental conditions of formation. Yet, the impurity contents of biominerals are subject to “vital effects” that can induce large offsets from equilibrium values (7). These “vital effects” are believed to have kinetic and taxonomic origins, but the mechanistic basis for measured offsets is not well understood. A complicating factor is that mineralization is isolated from the external environment and occurs within an organic-rich matrix (10) whose roles in mineralization are recognized but difficult to assess. At sites of calcification, this microenvironment contains complex assemblages of proteins and polysaccharides (10) whose structures and amino acid sequences are species-specific (5, 10–12). Moreover, calcifying macromolecules are unusually enriched in the carboxyl-rich acidic amino acids aspartate and glutamate (10, 11), and their presence is im-

pllicated in modulating biomineral formation (13, 14). Similarly, a number of widely cited studies of nonskeletal carbonates have questioned whether humic and protein substances (also enriched in acidic amino acids) in marine sedimentary environments could influence mineralization (2, 3).

Many observations and in vitro experimental studies show that aspartate-rich biomolecules

enhance calcite growth (11, 13, 14). Indeed, a recent study found that nanomolar concentrations of acidic amino acids, peptides, and full proteins accelerate calcite growth rate (up to 25 times) by a relation that correlates with the hydrophilicity of biomolecules (14), a measure of their interactions with water. These insights led us to hypothesize that because (i) cation incorporation is the rate-limiting step to growth (15) and (ii) Mg is more strongly solvated than Ca (16), then rate-modifying peptides could also lower the desolvation barrier to Mg incorporation relative to Ca and thereby alter Mg content.

To test this idea, we grew calcite under controlled chemical conditions within a flow-through cell of an atomic force microscope (AFM). Growth was observed in situ for the duration of each experiment while kinetic and surface thermodynamic properties were simultaneously measured. We monitored the propagation of steps at dislocation hillocks to observe the growth process during each treatment. Using established methods (17–19), we conducted experiments at a constant supersaturation (defined with respect to pure calcite),  $\sigma$ , of 1.6 where

$$\sigma = \ln(a_{\text{Ca}^{2+}} a_{\text{CO}_3^{2-}} / K_{\text{sp}}) \quad (1)$$

such that  $a_i$  is the activity of species  $i$ , and  $K_{\text{sp}}$  is the equilibrium solubility constant ( $10^{-8.48}$  for pure calcite at 25°C). The  $\text{Ca}^{2+}:\text{CO}_3^{2-}$  ratio was

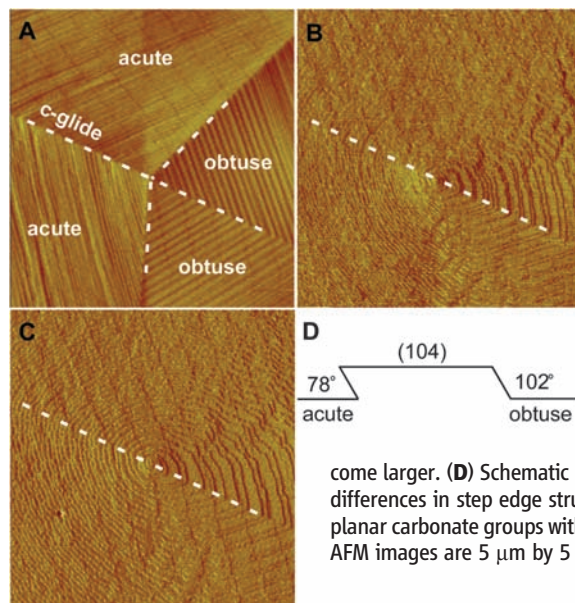


**Fig. 1.** AFM images of calcite growth hillocks. **(A)** In the absence of Mg or peptide modifiers, growth hillocks develop by the propagation of straight steps that lack visible roughening. The  $c$ -glide plane bisects two types of symmetrically equivalent step edges that define the obtuse and acute step directions to give four hillock flanks. **(B)** With  $3 \times 10^{-4}$  M Mg, step edges, particularly on acute flanks, become roughened and hillock morphology is elongated parallel to the  $c$ -glide axis. **(C)** With peptide and  $3 \times 10^{-4}$  M Mg, acute step edges are roughened as before, and the terrace widths become larger. **(D)** Schematic cross section of the step risers illustrates differences in step edge structure that arise from the orientation of planar carbonate groups with respect to the (104) growth surface. All AFM images are  $5 \mu\text{m}$  by  $5 \mu\text{m}$ .

<sup>1</sup>Department of Geosciences, Virginia Tech, Blacksburg, VA 24061, USA. <sup>2</sup>Chemistry and Materials Science Directorate, Lawrence Livermore National Lab, Livermore, CA 94551, USA. <sup>3</sup>Department of Applied Science, University of California–Davis, Davis, CA 95616, USA. <sup>4</sup>Department of Biological Sciences, University of Delaware, Newark, DE 19716, USA.

\*To whom correspondence should be addressed. E-mail: dove@vt.edu (P.M.D.) and aestephe@vt.edu (A.E.S.)

held at 1:1 to maximize growth rate (15), pH was constant at 8.5, and Mg concentrations were varied from 0 to  $4 \times 10^{-4}$  M. Control experiments established an inorganic baseline for comparisons to calcites grown in solutions containing 10 nM  $(\text{Asp}_3\text{Gly})_6\text{Asp}_3$ , a synthetic 27-amino acid peptide. This biomolecule was chosen for its similarity to Asp-rich peptide sequences found in proteins isolated from sites of calcification (11). The 10 nM concentration was selected to maximize the rate-enhancing effect without visibly roughening step edges at the micrometer scale (14). For experiments at the highest Mg concentration ( $4 \times 10^{-4}$  M), where slow growth made measurements difficult, peptide concentration was reduced to 1 nM.

In the absence of Mg or peptides, growth hillocks form by propagation of straight steps along four crystallographically defined directions (Fig. 1A). When Mg was introduced to the solution, steps along acute directions showed characteristic (18) rounding and roughening (Fig. 1B). With the addition of peptide, step spacing increased but hillock morphology did not appreciably change (compare Fig. 1, B and C).

The Mg contents of AFM-prepared overgrowths were determined by time-of-flight-secondary ion mass spectrometry (ToF-SIMS) with a calibration curve established from NIST (National Institute of Standards and Technology) glass stan-

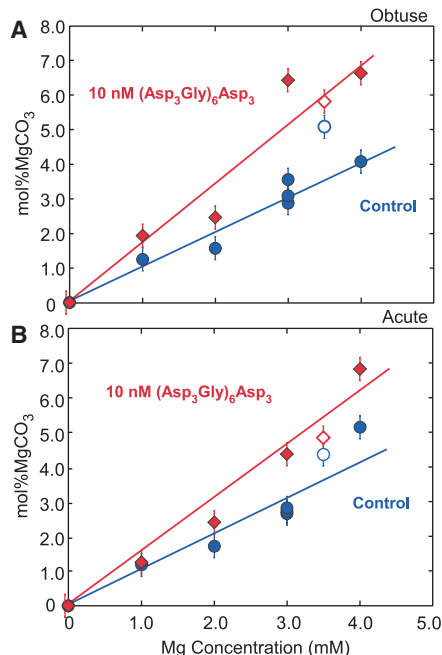


**Fig. 2.** Growth solutions containing the Asp-rich polypeptide increase the Mg content up to 3 mol%  $\text{MgCO}_3$  into calcite overgrowths (red trend line) compared to the inorganic controls (blue trend line). The enhancement due to peptide is greater on flanks comprising obtuse steps (A) than on those comprising acute steps (B). Open symbols show data with larger uncertainties. They are reported in the figure but are not included in the regressions (Eqs. 2a and 2b, and 3a and 3b).

dards by inductively coupled plasma mass spectrometry. Control experiments established a baseline relation between Mg content and Mg concentration ( $[\text{Mg}]$ ) in solution:

$$\text{mol\% MgCO}_3 \text{ obtuse} = 1.02 \pm 0.34 [\text{Mg, mM}] \quad (2a)$$

$$\text{mol\% MgCO}_3 \text{ acute} = 1.03 \pm 0.08 [\text{Mg, mM}] \quad (2b)$$

Obtuse and acute step edge directions incorporate Mg such that the contents of hillock flanks exhibit a linear dependence on solution concentration that is the same within experimental errors (Fig. 2, A and B). This is consistent with previous studies showing that transport conditions influence Mg uptake (20). In contrast to growth in diffusion-limited environments that results in differential uptake, acute and obtuse steps incorpo-

rate similar amounts of Mg during growth under surface reaction-limited conditions (17, 20).

Calcites grown in the presence of Asp-rich peptide incorporate 50 to 75% more Mg (Fig. 2, A and B) by the relations

$$\text{mol\% MgCO}_3 \text{ obtuse, peptide} = 1.75 \pm 0.34 [\text{Mg, mM}] \quad (3a)$$

$$\text{mol\% MgCO}_3 \text{ acute, peptide} = 1.55 \pm 0.08 [\text{Mg, mM}] \quad (3b)$$

such that Mg content is increased by up to ~3 mol%  $\text{MgCO}_3$  at the highest solution concentration of Mg and indicates preferential uptake across obtuse steps.

Insights into the origin of this behavior are found in kinetic measurements of step propagation rates,  $v$  ( $\text{nm s}^{-1}$ ). For calcite growth at  $\sigma = 1.6$ , step velocity is given by

$$v = \omega\beta (a_{\text{Ca}^{2+}} - a_{\text{Ca}^{2+e}}) \quad (4)$$

where step velocity ( $v$ ,  $\text{nm s}^{-1}$ ) is given by the molecular volume of calcite ( $\omega$ ,  $6.13 \times 10^{-23} \text{ cm}^3$  per molecule), the kinetic coefficient ( $\beta$ ), the local activity of  $\text{Ca}^{2+}$  at the growing surface ( $a_{\text{Ca}^{2+}}$ ), and the equilibrium  $\text{Ca}^{2+}$  activity for the crystal that forms and is the value of calcium activity for which step speed extrapolates to zero ( $a_{\text{Ca}^{2+e}}$ ) (17, 18). Calcite growth velocity decreased with increasing Mg concentration in the inorganic control solutions (Fig. 3A), as expected (18).

In contrast, growth in solutions that also contain peptide offset growth rate to 25 to 50% faster velocities (Fig. 3A). This enhanced growth rate could be responsible for the increased Mg contents because studies have shown that impurity contents correlate with faster growth (21), though no mechanism for this correlation has yet been established. Elhadj *et al.* (14) showed that biomolecule-induced increases in growth rate arise from increases in  $\beta$ . The magnitude of  $\beta$  is controlled by two primary factors: (i) density of kink sites along the step,  $n_k$ ; and (ii) net probability of attachment to a site, which we write as  $\exp(-E_k/kT)$ , where  $k$  = Boltzmann's constant,  $T$  is temperature, and  $E_k$  is an effective barrier to attachment (17) of Ca or Mg at a kink such that

$$\beta \sim n_k \exp(-E_k/kT) \quad (5)$$

Assuming that  $v$  remains linear versus  $(a - a_e)$  in the presence of impurities, which is documented for the range of Mg (18) and value of  $\sigma$  used here (18), then we must conclude that  $n_k$  is a constant (19), although it may be reduced in magnitude relative to the pure system when impurities bind to the step. Thus, under these conditions,  $n_k$  is at its maximum value and impurities can only decrease  $n_k$  by blocking active kinks (22).

Allowing these constraints, the most likely origin of enhanced  $\beta$  is reductions in  $E_k$ . This interpretation is evidenced by a previous study showing that biomolecules promote calcite growth in proportion to their hydrophilic character (14). Analysis of those data suggests that acidic bio-

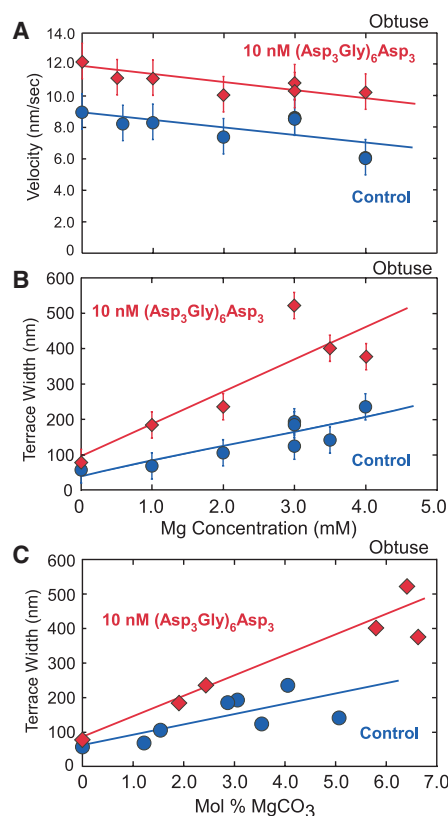


**Fig. 3.** Measurements of calcite growth show that (A) the rate of step propagation in the presence of peptides (red) is 25 to 50% faster than in the presence of inorganic controls (blue) for experimental conditions that are otherwise the same. (B) Terrace widths increase with increasing solution  $[\text{Mg}]$ , reflecting the formation of an increasingly soluble Mg-enriched overgrowth (compare to Fig. 2) and the consequent decrease in apparent supersaturation of the solid solution. (C) Terrace widths increase with Mg content. The offset between trends for the inorganic control (blue) and the peptide-bearing experiments (red) demonstrates that the biomolecules increase the step edge energy of calcite by 20 to 80%.

molecules create a lower-energy pathway for desolvating strongly hydrated cations as they approach the growing step edge (14). A similar mechanism was invoked to explain Mg uptake into calcites grown in alcohol-water mixtures (23) and was supported by molecular dynamics simulations showing that aspartic acid monomers enhance the rate of  $\text{Ba}^{2+}$  desolvation in the barite ( $\text{BaSO}_4$ ) system (24). Recent AFM observations of calcium oxalate monohydrate show that acidic biomolecules are weakly attracted to the surface and appear to serve as nutrient sources by promoting faster growth as steps propagate beneath the biomolecules (25). When one considers the extent of cation interactions with the acidic domains of biomolecules as a proxy for their ability to attract and desolvate cations, a plausible mechanistic picture emerges whereby biomolecules facilitate the uptake, desolvation, and transport of cations from bulk solution to the mineral surface.

Although this study cannot fully assess the physical model for enhancement, we can conclude that peptides affect Mg more strongly than Ca. If this peptide-induced perturbation were equivalent, the Mg/Ca ratio would be unchanged. Our analysis suggests that the only way to increase the proportion of Mg is to induce a drop in the barrier to Mg uptake that is greater than that for Ca. This can be understood by comparing the enthalpy of dehydration,  $\Delta H^\circ_{\text{rxn}}$ , for  $\text{Mg}^{2+}$  ( $-1882$  kJ/mol) versus  $\text{Ca}^{2+}$  ( $-1569$  kJ/mol) at  $25^\circ\text{C}$  (16). If, for example, biomolecules reduce  $\Delta H^\circ_{\text{rxn}}$  by 10%, then the energy barrier is reduced by almost 190 kJ/mol for Mg but only 157 kJ/mol

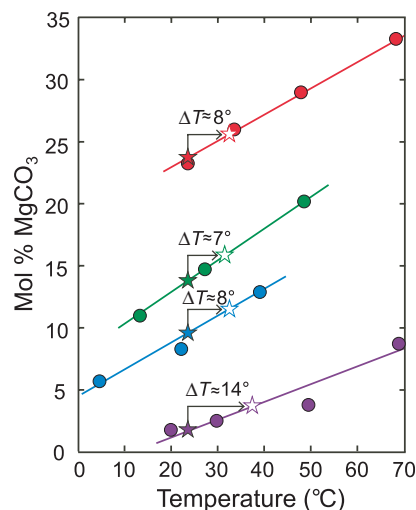


**Fig. 4.** Published correlations between Mg content and temperature show that if biomolecules induce a modest 2 mol% increase in Mg content, the corresponding temperature offset could be as much as  $7^\circ$  to  $14^\circ\text{C}$ . The different ionic strengths and supersaturations used in these studies do not allow a direct prediction, but only a general comparison. Legend: purple: Chilingar, 1962 (30); blue: Mucci, 1987 (31); green: Fuchtbauer and Hardie, 1976 (32); and red: Katz, 1973 (33).

for Ca. This kind of analysis raises two questions: (i) What is the “real” equilibrium distribution of Mg in calcite? Our findings suggest that Mg contents must be highly limited by kinetic factors. (ii) Do biomolecules also modify the hydration properties of other IIA cations and thus also modulate their incorporation? If true, this suggests the potential for selectively applying macromolecules during controlled materials synthesis to tune impurity or dopant levels.

Measurements of terrace width, or spacing between steps (Fig. 3C), indicate that surface thermodynamic properties of calcite may also be modified by peptides. Terrace width,  $\lambda$ , is controlled by the Gibbs-Thomson relation through

$$\lambda = (2.04 \omega \alpha) / kT\sigma \quad (6)$$

where  $\alpha$  = step edge free energy per unit step height (18). Though  $\lambda$  increases with increases in  $\omega$  and/or decreases in  $\sigma$ , we deduce here that  $\alpha$  is the origin of this effect. First, we assume changes in the molecular volume of calcites containing 0 to 6 mol% Mg are small relative to increases in  $\lambda$ . Next, we consider the influence of  $\sigma$  on  $\lambda$ . When the solid contains sufficiently high amounts of Mg,  $\sigma$  is reduced through increases in the apparent solubility (Eq. 1) (26, 27). However, comparisons to a previous study (18) show that the ratio of terrace widths for the peptide-bearing and control experiments is far too large to be explained by reductions in  $\sigma$ ; that is, the  $K_{\text{sp}}$  of calcites containing up to 4 mol%  $\text{MgCO}_3$  are not sufficiently different to explain the differences in terrace width for the Mg contents reported here. The peptide could also influence local  $\sigma$  by binding with Ca to reduce  $a_{\text{Ca}^{2+}}$  (Eq. 1), but two quantitative measurements show that these peptides have negligible effects on  $a_{\text{Ca}^{2+}}$  (28, 29). Citrate, an inhibitor with three carboxylic groups, does not measurably modify  $\sigma$  for calcium oxalate monohydrate systems until citrate concentrations are  $\geq 2$   $\mu\text{M}$ , and no change can be discerned below 10  $\mu\text{M}$  (28). Moreover, a study of calcite that used large amounts of Asp1 (29) indicates that nanomolar concentrations of  $(\text{Asp}_3\text{Gly})_6\text{Asp}_3$  are unlikely to substantially reduce  $\sigma$ . Even if every carboxylic of this 27-amino acid peptide acted independently, we would expect no effect for peptide concentrations of  $\leq 1$   $\mu\text{M}$ . Therefore, wider terraces that develop in peptide-bearing solutions must be due, at least in part, to increased  $\alpha$ . This is consistent with evidence that aspartate monomers also induce small increases in  $\alpha$  (28).

Our findings also raise new questions regarding carbonate mineralization and interpretations of their formation environments. In particular, do biomolecules substantially offset Mg signatures in natural calcites relative to the amounts attributed to temperature differences? Assuming a modest increase of 2.0 mol%  $\text{MgCO}_3$ , comparisons to published studies (30–33) show that an equivalent Mg enhancement corresponds to an offset of  $7^\circ$  to  $14^\circ\text{C}$  (Fig. 4). This crude compar-

ison is not a prediction but nonetheless illustrates that because the growth enhancement is specific to biomolecule chemistry (14) and acidic biomolecules induce greater Mg contents, perhaps some signatures are altered by macromolecule chemistry. These findings suggest that the basic assumption of paleotemperature reconstruction models would be degraded if the vital effect due to biomolecules were to change over time. One could also ask if biomolecules are a source of the vital effects long reported for stable isotopic signatures (34).

This study may also provide mechanism-based insights into factors that influence the stability of carbonate minerals in biological and sedimentary settings (35). Marine sediments contain organic matter that is frequently enriched in aspartate and glutamate (3). Because carbonate surfaces in these environments interact preferentially with aspartate-rich domains (3), findings that Asp1 and  $(\text{Asp}_3\text{Gly})_6\text{Asp}_3$  have compound-specific effects on  $\alpha$  suggest a means by which biomolecule chemistry could passively influence polymorph selection. Although step edge energy cannot be equated to surface energy, the generally accepted practice is to estimate step edge energy as the surface energy for the face that defines the step riser (Fig. 1D) times the step height. So, greater step edge energy implies greater surface energy. The increased surface energy of a phase makes nucleation of that phase less likely to occur. Thus, one polymorph becomes favored over another (36). Hence, if biomolecules increase  $\alpha_{\text{calcite}}$  more than  $\alpha_{\text{aragonite}}$ , organics could induce preferential formation of aragonite. Aside from the well-documented influence of Mg on the stability of carbonate polymorphs, shifts in  $\alpha$  could offer an alternative explanation for occurrences of aragonite needles in carbonate muds containing proteinaceous compounds enriched in acidic amino acids (2, 3). Formation of skeletal and inorganic carbonates alike may be better understood by considering biomolecule influences on kinetics and thermodynamics of mineral growth and stability.

## References and Notes

1. A. P. Vinogradov, *The Elementary Chemical Composition of Marine Organisms* (Yale University, New Haven, CT, 1953).
2. R. A. Berner, J. T. Westrich, R. Graber, J. Smith, C. S. Martens, *Am. J. Sci.* **278**, 816 (1978).
3. P. W. Carter, R. M. Mitterer, *Geochim. Cosmochim. Acta* **42**, 1231 (1978).
4. R. L. Folk, *J. Sediment. Petrol.* **44**, 40 (1974).
5. S. Bentov, J. Erez, *Geochem. Geophys. Geosyst.* **7**, Q01P08 (2006).
6. H. Elderfield, G. Ganssen, *Nature* **405**, 442 (2000).
7. D. W. Lea, in *The Oceans and Marine Geochemistry*, H. Elderfield, Ed., vol. 6 of *Treatise on Geochemistry*, H. D. Holland, K. K. Turekian, Eds. (Elsevier-Perigamon, Oxford, 2003), pp. 365–390.
8. J. A. D. Dickson, *Science* **298**, 1222 (2002).
9. S. M. Stanley, L. A. Hardie, *Palaeogeogr. Palaeoclimatol. Palaeoecol.* **144**, 3 (1999).
10. L. Addadi, S. Weiner, *Proc. Natl. Acad. Sci. U.S.A.* **82**, 4110 (1985).
11. L. Addadi, A. Berman, J. Moradianoldak, S. Weiner, *Croat. Chem. Acta* **63**, 539 (1990).

12. A. Puverel *et al.*, *Comp. Biochem. Physiol. B Biochem. Mol. Biol.* **141**, 480 (2005).
13. G. Fu, S. R. Qiu, C. A. Orme, D. E. Morse, J. J. De Yoreo, *Adv. Mater.* **17**, 2678 (2005).
14. S. Elhadji, J. J. De Yoreo, J. R. Hoyer, P. M. Dove, *Proc. Natl. Acad. Sci. U.S.A.* **103**, 19237 (2006).
15. M. Kowacz, C. Putnis, A. Putnis, *Geochim. Cosmochim. Acta* **71**, 5168 (2007).
16. J. E. Huheey, *Inorganic Chemistry: Principles of Structure and Reactivity* (Harper and Row, New York, ed. 3, 1983).
17. L. E. Wasylenki, P. M. Dove, J. J. De Yoreo, *Geochim. Cosmochim. Acta* **69**, 4227 (2005).
18. K. J. Davis, P. M. Dove, J. J. De Yoreo, *Science* **290**, 1134 (2000).
19. H. H. Teng, P. M. Dove, C. A. Orme, J. J. De Yoreo, *Science* **282**, 724 (1998).
20. R. J. Reeder, *Geochim. Cosmochim. Acta* **60**, 1543 (1996).
21. R. B. Lorens, *Geochim. Cosmochim. Acta* **45**, 553 (1981).
22. A. A. Chernov, *Theor. Technol. Aspects Cryst. Growth* **276-2**, 57 (1998).
23. G. Falini, M. Gazzano, A. Ripamonti, *Chem. Commun.* **9**, 1037 (1996).
24. S. Piana, F. Jones, J. D. Gale, *J. Am. Chem. Soc.* **128**, 13568 (2006).
25. J. J. De Yoreo, paper presented at the 233rd Annual Meeting of the American Chemical Society, Chicago IL, 25 to 29 March 2007.
26. J. M. Astilleros, C. M. Pina, L. Fernández-Díaz, A. Putnis, *Geochim. Cosmochim. Acta* **67**, 1601 (2003).
27. M. Prieto, J. M. Astilleros, C. M. Pina, L. Fernández-Díaz, A. Putnis, *Am. J. Sci.* **307**, 1034 (2007).
28. M. L. Weaver *et al.*, *J. Cryst. Growth* **306**, 135 (2007).
29. C. A. Orme *et al.*, *Nature* **411**, 775 (2001).
30. G. V. Chilingar, *Bull. South. Calif. Acad. Sci.* **61**, 45 (1962).
31. A. Mucci, *Geochim. Cosmochim. Acta* **51**, 1977 (1987).
32. H. Fuchtbauer, L. A. Hardie, *Geol. Soc. Am. Abstr.* **8**, 87719 (1976).
33. A. Katz, *Geochim. Cosmochim. Acta* **37**, 1563 (1973).
34. S. Epstein, *Geol. Soc. Am. Bull.* **62**, 417 (1951).
35. J. W. Morse, A. J. Andersson, F. T. Mackenzie, *Geochim. Cosmochim. Acta* **70**, 5802 (2006).
36. A. Navrotsky, *Proc. Natl. Acad. Sci. U.S.A.* **101**, 12096 (2004).
37. We thank J. F. Read and D. Rimstidt for thoughtful discussions. This research was supported by awards to P.M.D. from the NSF (grant OCE-052667) and U.S. Department of Energy (grant FG02-00ER15112). This work was also performed under the auspices of the U.S. DOE by an award to J.D.Y. at the University of California, Lawrence Livermore National Laboratory, under Contract No. W-7405-Eng-48. Opinions, findings, and conclusions or recommendations expressed in this material are those of the authors and do not necessarily reflect the views of the NSF or DOE.

21 April 2008; accepted 26 September 2008  
10.1126/science.1159417

## Trampoline Effect in Extreme Ground Motion

Shin Aoi,\* Takashi Kunugi, Hiroyuki Fujiwara

In earthquake hazard assessment studies, the focus is usually on horizontal ground motion. However, records from the 14 June 2008 Iwate-Miyagi earthquake in Japan, a crustal event with a moment magnitude of 6.9, revealed an unprecedented vertical surface acceleration of nearly four times gravity, more than twice its horizontal counterpart. The vertical acceleration was distinctly asymmetric; the waveform envelope was about 1.6 times as large in the upward direction as in the downward direction, which is not explained by existing models of the soil response. We present a simple model of a mass bouncing on a trampoline to account for this asymmetry and the large vertical amplitude. The finding of a hitherto-unknown mode of strong ground motion may prompt major progress in near-source shaking assessments.

The deployment of high-density seismograph networks has contributed to recent discoveries concerning ground shaking and complex wave propagation (1–3) and to the development of ShakeMap, a tool for real-time seismology and earthquake hazard mitigation (4, 5). As more and

more near-source data have become available, the stockpile of extreme ground motion observations has become ever larger, with potentially rich implications for earthquake engineering and building design.

Japan has deployed and maintained nationwide networks of strong motion seismographs (6–9),

with about 1800 stations. A station of the KiK-net (10) recorded ground acceleration exceeding four times gravity (11), the largest ever reported to date, during the 14 June 2008 Iwate-Miyagi earthquake, a reverse-fault type crustal event extending roughly 30 km in strike and 20 km in dip directions (Fig. 1A). The motion in question was recorded at the IWTH25 (West Ichinoseki) station, located on the hanging-wall side of the fault (12), 3 km southwest of the epicenter. The IWTH25 station is equipped with three-component accelerometers, installed at both the free surface and the bottom of a 260-m borehole (Fig. 1B). It lies in a volcanic zone where volcanoclastic rocks, such as tuff breccia, are covered with a surface layer of river terrace deposits (S-wave velocity 430 m/s in the shallowest surface layer) (fig. S1A).

National Research Institute for Earth Science and Disaster Prevention, 3-1 Tennodai, Tsukuba, Ibaraki 305-0006, Japan.

\*To whom correspondence should be addressed. E-mail: aoi@bosai.go.jp

